CHLORIDE PENETRATION PREDICTION IN CONCRETE THROUGH AN EMPIRICAL MODEL BASED ON CONSTANT FLUX DIFFUSION

G. de Vera[1], M. A. Climent[2], E. Viqueira[3], C. Antón[4], M. P. López[5]

ABSTRACT

An empirical model based on constant flux is presented for chloride transport through concrete in atmospherical exposure conditions. A continuous supply of chlorides is assumed as a constant mass flux at the exposed concrete surface. Model is applied to experimental chloride profiles obtained from a real marine structure, and results are compared with the classical error function model. The proposed model shows some advantages. It yields a better predictive capacity than the classical error function model. The previously observed chloride surface concentration increases are compatible with the proposed model. Nevertheless, the predictive capacity of the model can fail if the concrete microstructure changes with time. The model seems to be appropriate for well-maturated concretes exposed to a marine environment in atmospherical conditions.

Keywords: Chloride, Diffusion, Long-term performance, Modeling, Marine environment.

INTRODUCTION

Chloride penetration prediction is necessary or convenient during the project and exploitation phases of reinforced or pre-stressed concrete structures exposed to salt laden environments, in order to assess the full or residual service-life time of the structure in relation to steel reinforcement corrosion.

[1]Departament d'Enginyeria Civil, Universitat d'Alacant, Ap. 99, 03080 Alacant, Spain. Corresponding author

[2]Departament d'Enginyeria Civil, Universitat d'Alacant, Ap. 99, 03080 Alacant, Spain

[3]Departament d'Enginyeria Civil, Universitat d'Alacant, Ap. 99, 03080 Alacant, Spain

[4]Departament d'Enginyeria Civil, Universitat d'Alacant, Ap. 99, 03080 Alacant, Spain

[5]Departament d'Enginyeria Civil, Universitat d'Alacant, Ap. 99, 03080 Alacant, Spain

For concrete structures exposed to marine atmospheric, splash or tidal zones, and also for deicing salt exposure conditions, concrete is not fully saturated with liquid, rather the material experiences wetting and drying periods, leading to variable and non-homogeneous degrees of water saturation of the material. There exist several physical models intending to predict the evolution of the ion penetration through materials by considering as accurately as possible the physical-chemical processes having an influence on the ionic transport. Some of them are single ion models, considering only the main deleterious species, for instance chloride (Cl^-) ion, and taking into account the different acting transport mechanisms, i.e. diffusion and convection in the case of unsaturated concrete (Saetta et al. 1993; Martín-Pérez et al. 2001; Meijers et al. 2005; Guzmán et al. 2011). Other multiionic models take into account the electrochemical couplings between the ions present in the inner electrolyte of the concrete pore solution and their effect on ionic transport and on other concrete properties (Marchand 2001; Samson et al. 2005; Nguyen et al. 2008; Baroghel-Bouny et al. 2011).

From a practical point of view, when dealing with chloride penetration prediction, concrete codes (Ministerio de Fomento 2008) usually recommend simplified models based on the empirical use of Fick's second law of diffusion, with the boundary condition of constant chloride content at the surface of concrete. The chloride profile is given then by:

$$c(x,t) = C_0 + (C_S - C_0)\text{erfc}\left(\frac{x}{2\sqrt{Dt}}\right) \tag{1}$$

Where $c(x,t)$ is chloride concentration as a function of depth from surface x and time t, C_0 is the initial (background) chloride concentration and erfc is the complement of the error function. These models use two main parameters: the chloride diffusion coefficient, D, and the surface chloride concentration, C_S, which are, in principle, supposed to be constant. Nevertheless, sometimes it is considered a progressive decrease of D with time (Ministerio de Fomento 2008; ACI Committee 365 2009), and a progressive build-up of C_S up to a certain age (ACI Committee 365 2009). Other researchers have also considered the annual change

in surface chloride concentration and its effect on the diffusion process (Cheung et al. 2009).

The ability to adopt appropriate values for C_S is a key issue to predict adequately the future Cl$^-$ penetration (Andrade et al. 2006). Nevertheless, it is difficult to assign values for C_S since it changes with time (Uji et al. 1990; Song et al. 2008; Ann et al. 2009), and because it depends not only on the environmental conditions, i.e. salt load, but also on the composition of concrete (Bamforth 1999), due to the different chloride fixation capacity of each binder (Yuan et al. 2009) . So, the C_S parameter cannot be deduced only from environmental parameters. It is only possible to assign reliable values for C_S on the basis of experimental data, i.e. Cl$^-$ content profiles obtained with similar concrete composition and in similar locations.

In this work the authors have used a simplified diffusion model based on the constant flux boundary condition, where the main parameters are the diffusion coefficient and the flux, or the amount of Cl$^-$ ingressed through a unit surface of concrete in the unit time, J. This boundary condition leads to an increase of C_S with the square root of time, which is in good agreement with experimental observations in reinforced concrete aerially exposed to marine environment (Uji et al. 1990; Costa and Appleton 1999b). Finally, another interesting aspect to consider is that, on the basis of published results (Meira et al. 2007), there is a possibility of finding relationships between the amount of Cl$^-$ ingressed in concrete and typical environmental parameters of the marine environment, such as the dry Cl$^-$ deposition, measured as per the wet-candle device (ASTM G140 1996) or the K3-type device (Lee and Moon 2006). Nevertheless, further research is required to ascertain this possibility, and also it is reasonable to suppose that these relationships will be dependent on concrete composition.

This model has been mentioned before and suggested to be used for the atmospheric marine or de-icing salt environments (Uji et al. 1990; ACI Committee 365 2000; Ann et al. 2009). But, to the authors' knowledge, there has been no report on the application of the model to experimental data obtained from concrete structures at different ages, which is necessary to assess its capabilities regarding Cl$^-$ penetration prediction.

The objective of this work is to provide some initial data on the application of the model to Cl$^-$ content profiles obtained from the aerial part of the concrete structure of a dock of the Alacant harbour, in South-East Spain. The exposure conditions correspond to an atmospheric Mediterranean marine environment, and the data bases correspond to ages of 13 and 20 years of the structure.

PROPOSED MODEL

Chloride transport is described by mass balance equation (2) and diffusion equation (3). A constant D value is assumed.

$$\frac{\partial c(x,t)}{\partial t} + \frac{\partial J(x,t)}{\partial x} = 0 \tag{2}$$

$$J(x,t) = -D\frac{\partial c(x,t)}{\partial x} \tag{3}$$

Initial condition is represented by:

$$c(x,0) = C_0 \tag{4}$$

I. e., the initial (background) chloride concentration value is C_0 $(kgCl^-/m^3 concrete)$. This is the same initial condition as in (1).

Boundary conditions are given by the exposure conditions. In an atmospheric exposure, chloride reaches surface in water droplets brought by wind. Considering an approximately constant supply of droplets we assume that chloride flux J $(kgCl^-/((m^2 surface)\cdot s))$ arriving to the surface is constant. In cold weather where de-icing salts are used, this boundary condition could be also acceptable (ACI Committee 365 2000). This boundary condition is expressed as:

$$-D\left.\frac{\partial c(x,t)}{\partial x}\right|_{x=0} = J \tag{5}$$

Where J is a constant. The second boundary condition states that far enough from the

4

surface chloride has not yet arrived, and it is expressed as:

$$\lim_{x \to \infty} c(x,t) = C_0 \tag{6}$$

This boundary condition was also assumed in (1). Equations (2) and (3) with initial and boundary conditions (4), (5), and (6) are solved using the Laplace transform technique (see appendix) yielding the solution:

$$c(x,t) = C_0 + 2J\sqrt{\frac{t}{\pi D}}\exp\left(-\frac{x^2}{4Dt}\right) - \frac{Jx}{D}\text{erfc}\left(\frac{x}{2\sqrt{Dt}}\right) \tag{7}$$

Substituting $x = 0$ in (7) the surface concentration is obtained:

$$C_S(t) = C_0 + 2J\sqrt{\frac{t}{\pi D}} \tag{8}$$

The absorbed amount of chlorides $m \left(kgCl^-/m^2 surface\right)$ for the proposed model is given by (see appendix):

$$m(t) = Jt \tag{9}$$

Calculated profiles from both models (1) and (7) are compared in Figure 1. Selected values for these plots are: $D = 10^{-12}m^2/s$, $C_S = 10kg/m^3$, $J = 10^{-9}kg/(m^2s)$, and $C_0 = 0kg/m^3$. Surface concentration and absorbed amount of chlorides are also compared for both models in Figure 2.

EXPERIMENTAL

Concrete cores extracted from the Alacant harbour were studied (Viqueira 2009). Alacant is a Mediterranean city located in the south-east of Spain (38° 19' N – 0° 29' W). All samples had atmospherical marine exposure conditions and were taken from the dock 17. This structure was built in 1984 and samples were taken in 1997 and 2004, thus samples were taken after 13 and 20 years exposure respectively. Five concrete cores were extracted in 1997 at

5

different locations in dock 17. Exposure conditions of each location are summarized in Table 1. Five concrete cores were extracted in 2004 in the same locations as in 1997. According to the documentation, structure was fabricated with bulk concrete H-175 (MOPU 1982) and cement used was ordinary Portland cement P-350 (MOPU 1975). The following tests were performed following standard methods on concrete cores extracted from the studied structure: compressive strength, cement content quantification (Chinchón et al. 2004), bulk density, and porosity. Mean values, corresponding to at least three samples, are shown in Table 2.

Powder samples were obtained from the concrete cores by grinding (Vennesland et al. 2013). This technique allows obtaining powder samples in 2mm intervals. Powder samples were analysed to determine its total chloride contents. The method used was potentiometric titration with end-point detection by Gran's method (Climent et al. 1999; Climent et al. 2004). Thus, detailed chloride profiles were obtained. Bulk density (see Table 2) was also determined (ASTM C642-90) in order to refer chloride concentrations as $kgCl^-/m^3$ of concrete instead of mass percentages. The mean value of density obtained from several samples at both ages was $2150 kg/m^3$. This value was used in all calculations involving density.

Experimental profiles were fitted to both models, i. e. the well-known error function solution of Fick's second law (1), and the proposed model (7).

RESULTS AND DISCUSSION

Experimental profiles are shown in Figure 3 to Figure 7. Each figure is devoted to one location in dock 17. Experimental profiles obtained after 13 years of exposure time are plotted with circles while the ones obtained after 20 years exposure time are plotted with asterisks.

The presence of peaks can be observed in the experimental profiles of Figs. 3 to 7. Neither model (1) nor model (7) can predict the presence of peaks in the profiles (see Figure 1). This is a consequence of the fact that both models are empirical, so they can not

6

take into account all the physical phenomena involved in the chloride transport process. In an atmospherical exposure, wetting and drying cycles can occur near the surface and then chloride transport due to water absorption can happen. This mechanism has not been considered in the presented models, which only consider the diffusion mechanism. It can also be seen that in general peaks move inwards with time, although a different behaviour can be observed sometimes, see Figure 5. Transport between surface and the maximum is probably determined by convection processes (Kropp 1995) and the authors refer to this zone as convective zone, while the profile from the maximum inwards is probably due to diffusion processes and the authors refer to this zone as diffusive zone. The possibility of transient wetting-drying effects, mostly affecting concrete exposed to seawater splash, can explain the differences observed in the evolution of the instantaneous peak position inside the convective zone, Figure 5. Both models presented (1) and (7) do not take into account convective processes and they fail describing the profiles in the convective zone.

The experimental value of the chloride mean flux $\bar{J}$ has been calculated as:

$$\bar{J} = \frac{1}{t} \int_0^\infty (c(x,t) - C_0)dx \tag{10}$$

The integration in last equation has been done with the trapezoidal rule and all the data points of the experimental profiles have been used. A negligible amount of chloride is expected to be in the concrete when it was fabricated, and thus a value of $C_0 = 0 kg/m^3$ has been assumed in all cases. Table 3 shows the calculated chloride mean fluxes $\bar{J}$. It is interesting to note in Table 3 that experimental values of $\bar{J}$ increase when passing from 13 to 20 years exposure time. The absorbed mass of chlorides per unit area from model (1) is given by:

$$m(t) = 2(C_S - C_0)\sqrt{\frac{Dt}{\pi}} \tag{11}$$

7

Thus for the classical model (1) is expected a mean flux as:

$$\bar{J}(t) = \frac{m(t)}{t} = 2(C_S - C_0)\sqrt{\frac{D}{\pi t}} \tag{12}$$

I. e., mean flux decreasing proportional to $t^{-1/2}$, while for the proposed model (7) a constant J is expected. Values of Table 3 are less discordant with the proposed model (7) than with the classical error function model (1). A possible explanation for the increase of J with time could be the progressive modification of physical properties of concrete as its chloride concentration increases with time. It has been shown before for cement mortars increasingly contaminated with NaCl, and for the same water content, that the water vapour adsorption isotherm is progressively shifted to lower relative humidity values (Baroghel-Bouny et al. 2011). This implies that for cementitious materials the presence of salts in the pore system yields a decrease in the drying rate. Taking into account this, it is reasonable to suppose that as concrete in locations 1 to 5 progressively increase its chloride concentration, while the environmental conditions are approximately constant (considered in the long term), the surface layers of the material would progressively increase their degree of water saturation. This can modify the transport properties of concrete (Climent et al. 2002; de Vera et al. 2007), and eventually could modify the interaction between the concrete surface and the marine aerosol leading to a progressive increase of chloride uptake by concrete, i.e. an increment of the surface chloride flux J, which is the opposite behavior to that expected by the classical error-function diffusion model, see Equation (12).

Classical model (1) states that surface concentration C_S is constant. This point cannot be checked directly from the experimental profiles due to the presence of peaks.

Experimental data have been fitted to models (1) and (7) in order to obtain their parameters. Parameters for model (1) are D and C_S, while parameters for model (7) are D and J. The fit is done by looking for the parameters values that minimize the standard deviation defined in Equation (13), i. e. minimizing the mean difference between experimental and

8

calculated profiles.

$$\sigma = \sqrt{\frac{\sum\limits_{k=1}^{n}(C_k^{exp} - C_k^{calc})^2}{n}} \qquad (13)$$

Here n is the number of data points in the fitting, C_k^{exp} is the experimental chloride content of the data point number k, and C_k^{calc} is the corresponding value calculated with the used model. Only the points of the diffusive zone (from maximum inwards) have been used for the fitting, which is a common practice in profile treatment (Sandberg et al. 1998). The algorithm used to find the optimum parameter values is the Nelder-Mead method, which is a simplex algorithm. Calculations have been performed with MATLAB 6.1 software. Results are shown in Table 4 for the classical error function model (1), and in Table 5 for the proposed model (7). The correlation coefficient r used in both tables as an indicator of the goodness of the fitting, is the linear regression correlation coefficient of the plot of C_k^{calc} against C_k^{exp}.

Good correlation coefficients are found in Table 4 and Table 5. Fitted curves for 13 years exposure time are shown in Figure 3 to Figure 7. Model (1) is plotted with dotted lines and model (7) is plotted with dashed lines. The zone from the maximum inwards (diffusive zone), where data points have been used in the fitting, is very well represented with both models. Curves from both models differ in the outer zone (convective zone), yielding model (7) higher surface concentrations than model (1).

An interesting point observed in Table 4 and Table 5 is that diffusion coefficient for both models does not change a lot when passing from 13 years exposure time to 20 years. In general it remains approximately constant. The change in D observed in other cases has been attributed to changes in the porous structure (Costa and Appleton 1999a). This happens for concretes whose maturation is evolving. In the case here studied concrete is well maturated because samples were obtained after 13 and 20 years exposure time for an OPC concrete. Then a change in D is not expected and this fact is confirmed in Table 4 and Table 5. Nevertheless, a decrease of D in location 5 is observed. That could be attributed to the fact that the exposure conditions of location 5 changed, between the first (1997) and

9

the second (2004) campaigns of core extractions, due to construction works to enlarge the harbour, resulting in an increase of the distance between the sea line and location 5.

An increase of surface concentration C_S with time can be observed in Table 4 when applying the classical error function model (1). This behaviour has also been reported (Uji et al. 1990; Costa and Appleton 1999a) and can be attributed to exposure conditions. In this sense it is interesting to consider equation (8). The model (7) that we propose, with specific boundary conditions for atmospherical exposure, predicts an increase of surface concentration proportional to $\sqrt{t}$. This is in agreement with the experimentally observed behaviour (Uji et al. 1990; Costa and Appleton 1999b) as Equation (14), see Figure 3 to Figure 7.

$$
\begin{aligned}
C_S(t) &= C_{S1} \left(\frac{t}{1year} \right)^m \\
D(t) &= D_1 \left(\frac{1year}{t} \right)^n
\end{aligned}
\tag{14}
$$

Following Costa and Appleton (Costa and Appleton 1999b) experimental values of m in Equation (14) are in the range 0.54 to 0.69 when considering atmospherical exposure and in the range 0.37 to 0.69 when tidal and spray zones are also considered. This is in agreement with the value $m = \frac{1}{2}$ predicted by the proposed model (7).

In order to evaluate the predictive capacity of both models, they have been used to predict chloride profiles at 20 years exposure time from the measured profiles at 13 years. Parameters values obtained fitting chloride profiles at 13 years (2nd and 3rd columns in Table 4 and Table 5) have been introduced into equations (1) and (7) in order to predict chloride profiles at 20 years exposure time. These predicted profiles are shown in Figure 3 to Figure 7. Profiles predicted with model (1) are plotted with dash-dot lines, and profiles predicted with model (7) are plotted with solid lines. It can be seen that model (7) yields higher chloride concentrations than model (1). Predicted profiles can be compared with the experimental profiles at 20 years (plotted with asterisks). It can be observed in Figure 3 to Figure 7

that both models underestimate chloride concentrations. Nevertheless, differences between experimental and predicted profiles are lower when the proposed model (7) is used.

In order to get a parameter representing the predictive capacity of the models, the following has been calculated:

$$\alpha = \frac{I}{I_0} \tag{15}$$

Where:

$$I_0 = \int_{x_1}^{x_2} (C_{exp} - C_0)\, dx$$
$$I = \int_{x_1}^{x_2} |C_{calc} - C_{exp}|\, dx \tag{16}$$

Here C_{exp} is the experimental profile at 20 years, and C_{calc} is the predicted profile with the model used. Integration limits x_1 and x_2 are selected to include as much points as possible that correspond to the diffusive zone of both profiles (13 and 20 year). Integral I_0 represents the experimental absorbed amount of chlorides (kg/m^2), while I represents the difference between experimental and predicted profiles (measured also in kg/m^2). The lower is the I value, the better is the predictive capacity of the model. In order to compare values from different profiles the relative value α (15) has been calculated. Results are shown in Table 6.

Table 6 shows α values in the range 18% to 58%. Thus the predictive capacity of both models is not very bad, but it can not be considered good. It is worth noting that the proposed model (7) yields slightly lower α values, i. e. the model (7) has a slightly better predictive capacity than model (1).

Thomas and Bamforth (Thomas and Bamforth 1999) reported chloride profiles at different times for concretes exposed in the splash marine zone. Three concretes were used: concrete with ordinary Portland cement (PC), Portland cement with 30% fly ash replacement (P/PFA), and Portland cement with 70% slag replacement (P/GBS). Diffusion coefficient values were determined in reference (Thomas and Bamforth 1999) using model (1) and they are plotted against time in Figure 8A. Here, D values show a variation with time as described in Equation (14) for the concretes with additions. Reported values of n (see Equation (14)) are 0.7 for P/PFA and 1.2 for P/GBS. This dependency could be attributed to pozzolanic

11

activity, which would decrease porosity and the chloride ingress flux should also be affected. Mean flux values have been calculated with Equation (10) from profiles reported in (Thomas and Bamforth 1999), and results are plotted in Figure 8B. A decrease of $\bar{J}$ with time is observed, attaining a constant value after approximately 6 years of exposure.

The reduction of $\bar{J}$ and D with time observed in Figure 8 implies a limitation in the predictive capacity of model (7) when concrete is not well maturated. This fact is shown in Figure 9. An experimental profile (Thomas and Bamforth 1999) (concrete P/PFA) at time t_1 (circles in Figure 9) has been fitted to model (7) (dashed line). Parameters obtained have been used to predict the profile at time t_2 (solid line). The last one can be compared with the experimental profile at time t_2 (asterisks). In Figure 9A $t_1 = 0.5 year$ and $t_2 = 3 year$. The large difference between asterisks and solid line shows a strong fail in the prediction of this case. A possible explanation is that the microstructures of these concretes are probably changing greatly in this time range, as indicated by strong variations of the parameters D and J between 0.5 and 3 years, see Figure 8. In Figure 9B $t_1 = 6 year$ and $t_2 = 8 year$. In this case the microstructures of the concretes do not change practically, as indicated by the constancy of the parameters D and J in this time period, see Figure 8. Then, the prediction observed in Figure 9B is much better than that of Figure 9A. This seems to indicate that the model proposed in this work is appropriate for describing the chloride ingress and its evolution of well maturated concretes, whose microstructure is not evolving, exposed long time to atmospheric marine environments.

CONCLUSIONS

An empirical model based on constant flux is presented for describing the chloride transport through concrete exposed to atmospheric marine environment. Boundary conditions assumed are more realistic than the ones assumed in the classical error function model. A continuous supply of chlorides is assumed as a constant mass flux at the exposed concrete surface. The experimental chloride flux observed, for the studied concrete structure, is less discordant with the proposed model than with the classical error function model. Chloride

12

surface concentration is known to increase with time. This fact is compatible with the proposed model. Chloride profiles calculated at 20 years exposure time from data obtained at 13 years exposure time correlate better with the experimental chloride profiles at 20 years when the proposed model is used instead of the classical error function model. The proposed model, as well as the classical error function model, can not be applied to the outer concrete zone if transport mechanisms different from diffusion act. The predictive capacity of the proposed model can fail if the concrete microstructure changes with time. The model seems to be appropriate for well-maturated concretes exposed to a marine environment in atmospherical conditions. Nevertheless, it would be desirable to apply the proposed model to more experimental data in order to better validate the applicability and usefulness of the proposed model.

APPENDIX: MODEL DERIVATION

Diffusion equation (17) must be solved. This is a mass balance equation where transport is due to diffusion with a constant diffusion coefficient, i. e. Equation (3) substituted in Equation (2).

$$\frac{\partial c(x,t)}{\partial t} = D \frac{\partial^2 c(x,t)}{\partial x^2} \tag{17}$$

The following initial and boundary conditions are applied:

$$c(x,0) = C_0 \tag{18}$$

$$\lim_{x \to \infty} c(x,t) = C_0 \tag{19}$$

$$-D \left. \frac{\partial c(x,t)}{\partial x} \right|_{x=0} = J \tag{20}$$

These equations state that the flux is constant at surface (equation (20)), and that initial (background) concentration and concentration far enough from surface are equal to C_0.

The Laplace transform method is used in order to solve (17) subjected to (18), (19), and

13

(20). Applying the Laplace transform (see Table 7) to variable t in (17):

$$sC(x,s) - c(x,0) = D\frac{d^2 C(x,s)}{dx^2} \tag{21}$$

Substituting here the initial condition (18) and rearranging:

$$\frac{d^2 C(x,s)}{dx^2} - \frac{s}{D}C(x,s) = -\frac{C_0}{D} \tag{22}$$

In order to solve differential equation (22) the following homogeneous equation must be solved first:

$$\frac{d^2 C(x,s)}{dx^2} - \frac{s}{D}C(x,s) = 0 \tag{23}$$

Solution of (23) is:

$$C(x,s) = k_1 \exp\left(-x\sqrt{\frac{s}{D}}\right) + k_2 \exp\left(+x\sqrt{\frac{s}{D}}\right) \tag{24}$$

Where k_1 and k_2 are integration constants. The solution of the inhomogeneous equation (22) is then:

$$\begin{aligned} C(x,s) = \quad & k_1 \exp\left(-x\sqrt{\frac{s}{D}}\right) + k_2 \exp\left(+x\sqrt{\frac{s}{D}}\right) + \\ & +u_1(x) \exp\left(-x\sqrt{\frac{s}{D}}\right) + u_2(x) \exp\left(+x\sqrt{\frac{s}{D}}\right) \end{aligned} \tag{25}$$

Where $u_1(x)$ and $u_2(x)$ are given by the system:

$$\begin{bmatrix} e^{-x\sqrt{\frac{s}{D}}} & e^{+x\sqrt{\frac{s}{D}}} \\ -\sqrt{\frac{s}{D}}e^{-x\sqrt{\frac{s}{D}}} & +\sqrt{\frac{s}{D}}e^{+x\sqrt{\frac{s}{D}}} \end{bmatrix} \cdot \begin{bmatrix} \frac{du_1(x)}{dx} \\ \frac{du_2(x)}{dx} \end{bmatrix} = \begin{bmatrix} 0 \\ \frac{-C_0}{D} \end{bmatrix} \tag{26}$$

Solving and integrating (26) the folloeing expressions are obtained:

$$u_1(x) = \frac{C_0}{2s}e^{+x\sqrt{\frac{s}{D}}}$$

$$u_2(x) = \frac{C_0}{2s}e^{-x\sqrt{\frac{s}{D}}} \tag{27}$$

14

Substituting (27) in (25):

$$C(x,s) = k_1 \exp\left(-x\sqrt{\frac{s}{D}}\right) + k_2 \exp\left(+x\sqrt{\frac{s}{D}}\right) + \frac{C_0}{s} \tag{28}$$

Now Laplace transform is applied to boundary condition (19):

$$\lim_{x \to \infty} C(x,s) = \frac{C_0}{s} \tag{29}$$

The only way to accomplish this is making $k_2 = 0$ in (28), yielding:

$$C(x,s) = k_1 \exp\left(-x\sqrt{\frac{s}{D}}\right) + \frac{C_0}{s} \tag{30}$$

In order to get the other integration constant k_1 the Laplace transform is applied to the last boundary condition (20):

$$-D \left.\frac{dC(x,s)}{dx}\right|_{x=0} = \frac{J}{s} \tag{31}$$

The derivative of (30) is:

$$\left.\frac{dC(x,s)}{dx}\right|_{x=0} = -k_1\sqrt{\frac{s}{D}} \exp\left(-x\sqrt{\frac{s}{D}}\right)\Bigg|_{x=0} = -k_1\sqrt{\frac{s}{D}} \tag{32}$$

Substituting (32) in (31) and rearranging k_1 is obtained:

$$k_1 = \frac{J}{s^{3/2}\sqrt{D}} \tag{33}$$

And substituting it in (30):

$$C(x,s) = \frac{J}{s^{3/2}\sqrt{D}} \exp\left(-x\sqrt{\frac{s}{D}}\right) + \frac{C_0}{s} \tag{34}$$

15

Finally the inverse Laplace transform is applied to get the desired expression:

$$c(x,t) = C_0 + 2J\sqrt{\frac{t}{\pi D}}\exp\left(-\frac{x^2}{4Dt}\right) - \frac{Jx}{D}\text{erfc}\left(\frac{x}{2\sqrt{Dt}}\right)$$

(35)

It is interesting to determine surface concentration. Making $x = 0$ in (35) surface concentration is obtained:

$$C_S(t) = C_0 + 2J\sqrt{\frac{t}{\pi D}}$$

(36)

The absorbed amount of substance is given by:

$$m(t) = \int_0^\infty (c(x,t) - C_0)dx$$

(37)

Applying here the Laplace transform and taking into account (34):

$$\mathcal{L}\{m(t)\} = \int_0^\infty \left(C(x,s) - \frac{C_0}{s}\right)dx = \frac{J}{s^2}$$

(38)

Which inverse Laplace transform yields:

$$m(t) = Jt$$

(39)

I. e. absorbed mass per surface unit is proportional to time as expected for a constant flux J.

ACKNOWLEDGEMENTS

16

371   Investigador (FPI)" programme (reference BES-2011-046401).

REFERENCES

ACI Committee 365 (2000). *Service-life prediction: State-of-the-art report.* American Concrete Institute.

ACI Committee 365 (2009). *Life-365 Service Life Prediction Model and Computer Program for Predicting the Service Life and Life-Cycle Cost of Reinforced Concrete Exposed to Chlorides, version 2.0.1.* American Concrete Institute, Farmington Hills, Michigan, USA.

Andrade, C., Tavares, F., Castellote, M., Petre-Lazar, I., Climent, M. A., and de Vera, G. (2006). "Comparison of chloride models: the importance of surface concentration." *Proceedings of the 2nd Int. Symp. on "Advances in Concrete through Science and Engineering", Quebec City Canada*, J. Marchand, B. Bissonnette, R. Gagné, M. Jolin, and F. Paradis, eds., Bagneux, France, RILEM Publications pro051, 227–242.

Ann, K. Y., Ahn, J. H., and Ryou, J. S. (2009). "The importance of chloride content at the concrete surface in assessing the time to corrosion of steel in concrete structures." *Const Build Mat*, 23, 239–245.

ASTM C642-90. *Standard Test Method for Specific Gravity, Absorption, and Voids in Hardened Concrete.*

ASTM G140 (1996). *Standard test method for determining atmospheric chloride deposition rate by wet candle method.* ASTM International.

Bamforth, P. B. (1999). "The derivation of input data for modelling chloride ingress from eight-year UK coastal exposure trials." *Mag Concr Res*, 51(2), 87–96.

Baroghel-Bouny, V., Thiéry, M., and Wang, X. (2011). "Modelling of isothermal coupled moisture-ion transport in cementitious materials." *Cem Concr Res*, 41, 828–841.

Cheung, M., Zhao, J., and Chan, Y. (2009). "Service life prediction of RC bridge structures exposed to chloride environments." *J. Bridge Eng.*, 14(3), 164–178.

Chinchón, S., García, J., López Atalaya, M., Linares, A., and Vera, R. (2004). "Cement paste colouring in concretes." *Cem Concr Res*, 34, 1987–1991.

Climent, M. A., de Vera, G., López, J. F., Viqueira, E., and C.Andrade (2002). "A test

18

method for measuring chloride diffusion coefficients through nonsaturated concrete. Part I. The instantaneous plane source diffusion case." *Cem Concr Res*, 32(7), 1113–1123.

Climent, M. A., de Vera, G., Viqueira, E., and López, M. M. (2004). "Generalization of the possibility of eliminating the filtration step in the determination of acid-soluble chloride content in cement and concrete by potentiometric titration." *Cem Concr Res*, 34(12), 2291–2295.

Climent, M. A., Viqueira, E., de Vera, G., and López Atalaya, M. M. (1999). "Analysis of acid-soluble chloride in cement, mortar and concrete by potentiometric titration without filtration steps." *Cem Concr Res*, 29, 893–898.

Costa, A. and Appleton, J. (1999a). "Chloride penetration into concrete in marine environment. Part I: Main parameters affecting chloride penetration." *Mater and Struct*, 32, 252–259.

Costa, A. and Appleton, J. (1999b). "Chloride penetration into concrete in marine environment. Part II: Prediction of long term chloride penetration." *Mater and Struct*, 32, 354–359.

de Vera, G., Climent, M. A., Viqueira, E., Antón, C., and Andrade, C. (2007). "A test method for measuring chloride diffusion coefficients through partially saturated concrete. Part II. The instantaneous plane source diffusion case with chloride binding consideration." *Cem Concr Res*, 37(5), 714–724.

Guzmán, S., Gálvez, J. C., and Sancho, J. M. (2011). "Cover cracking of reinforced concrete due to rebar corrosion induced by chloride penetration." *Cem Concr Res*, 41, 893–902.

Kropp, J. (1995). "Chlorides in concrete." *Performance Criteria for Concrete Durability*, J. Kropp and H. K. Hilsdorf, eds., E & FN Spon, London, 138–164.

Lee, J. S. and Moon, H. Y. (2006). "Salinity distribution of seashore concrete structures in korea." *Build Environm*, 41, 1447–1453.

Marchand, J. (2001). "Modeling the behavior of unsaturated cement systems exposed to aggressive chemical environments." *Mater and Struct*, 34, 195–200.

426 Martín-Pérez, B., Pantazapoulou, S. J., and Thomas, M. D. A. (2001). "Numerical solution

427 of mass transport equations in concrete structures." *Computers and Structures*, 79, 1251–

428 1264.

429 Meijers, S. J. H., Bijen, J. M. J. M., de Borst, R., and Fraaij, A. L. A. (2005). "Computational

430 results of a model for chloride ingress in concrete including convection, drying-wetting

431 cycles and carbonation." *Mater and Struct*, 38(2), 145–154.

432 Meira, G. R., Andrade, C., Padaratz, I. J., Alonso, C., and Borba, Jr, J. C. (2007). "Chloride

433 penetration into concrete structures in the marine atmosphere zone — relationship between

434 deposition of chlorides on the wet candle and chlorides accumulated into concrete." *Cem*

435 *Concr Comp*, 29(9), 667–676.

436 Ministerio de Fomento (2008). *Instrucción de Hormigón Estructural EHE-08 (Structural*

437 *Concrete Code EHE-08)*. Madrid, Spain. (In Spanish).

438 MOPU (23 may 1975). *Real Decreto 1964/1975: Pliego de prescripciones técnicas generales*

439 *para la Recepción de Cemento (RC-75)*. Boletín Oficial del Estado (BOE), Madrid, Spain.

440 Ministerio de Obras Públicas y Urbanismo (In Spanish).

441 MOPU (24 july 1982). *Real Decreto 2252/1982: Instrucción para el proyecto y ejecución de*

442 *obras de hormigón en masa o armado (EH-82)*. Boletín Oficial del Estado (BOE), Madrid,

443 Spain. Ministerio de Obras Públicas y Urbanismo (In Spanish).

444 Nguyen, T. Q., Petković, J., Dangla, P., and Baroghel-Bouny, V. (2008). "Modelling of

445 coupled ion and moisture transport in porous building materials." *Constr Build Mat*,

446 22(11), 2185–2195.

447 Saetta, A. V., Scotta, R. V., and Vitaliani, R. V. (1993). "Analysis of chloride diffusion into

448 partially saturated concrete." *ACI Mater J*, 90(5), 441–451.

449 Samson, E., Marchand, J., Snyder, K. A., and Beaudoin, J. J. (2005). "Modeling ion and

450 fluid transport in unsaturated cement systems in isothermal conditions." *Cem Concr Res*,

451 35(1), 141–153.

452 Sandberg, P., Tang, L., and Andersen, A. (1998). "Recurrent studies of chloride ingress in

uncracked marine concrete at various exposure times and elevations." *Cem Concr Res*, 28(10), 1489–1503.

Song, H. W., Lee, C. H., and Ann, K. Y. (2008). "Factors influencing chloride transport in concrete structures exposed to marine environments." *Cem Concr Comp*, 30, 113–121.

Thomas, M. D. A. and Bamforth, P. B. (1999). "Modelling chloride diffusion in concrete. effect of fly ash and slag." *Cem Concr Res*, 29, 487–495.

Uji, K., Matsuoka, Y., and Maruya, T. (1990). "Formulation of an equation for surface chloride content of concrete due to permeation of chloride." *Proc. of the Third Int. Symp. on Corrosion of Reinforcement in Concrete*, C. L. Page, K. W. J. Treadaway, and P. B. Bamforth, eds., Society for the Chemical Industry, Warwickshire, UK, 258–267 (May).

Vennesland, Ø., Climent, M. A., and Andrade, C. (2013). "Recommendation of RILEM TC 178-TMC: Testing and modeling chloride penetration in concrete. methods for obtaining dust samples by means of grinding concrete in order to determine the chloride concentration profile." *Mater and Struct*, 46, 337–344.

Viqueira, E. (2009). "Contaminación por cloruros del hormigón debida a la interacción con los productos de combustión del PVC y a la exposición a una atmósfera marina (Concrete contamination by chlorides due to interaction with PVC combustion products and due to marine atmospherical exposure)." Ph.D. thesis, Universitat d'Alacant, Alacant (Spain). Only available in spanish.

Yuan, Q., Shi, C., De Schutter, G., Audenaert, K., and Deng, D. (2009). "Chloride binding of cement-based materials subjected to external chloride environment — A review." *Constr Build Mat*, 23, 1–13.

List of Tables

Location	Exposure condition	Wind	Seawater spray
1	Atmospheric	Protected	Low
2	Atmospheric	Protected	Low
3	Splash	Exposed	High
4	Atmospheric	Protected	Low
5	Atmospheric	Protected	Low

TABLE 1. Exposure conditions of locations.

Property	Value
Compressive strength (MPa)	25.6
Cement content (kg/m^3)	220
Bulk density (kg/m^3)	2150
Porosity (%)	15.8

TABLE 2. Properties of the studied concrete (mean values of at least three samples).

Location	$\bar{J}$ $[mgCl^-/(cm^2 \cdot year)]$	
	13 year	**20 year**
1	1.1081	1.4891
2	0.5947	0.9496
3	5.8453	6.4491
4	0.4956	0.8083
5	0.4098	0.5281

TABLE 3. Experimental fluxes of chloride determined from profiles.

Location	t = 13 year			t = 20 year		
	D	C_S	r	D	C_S	r
	$[10^{-12}m^2/s]$	$[kg/m^3]$	$[-]$	$[10^{-12}m^2/s]$	$[kg/m^3]$	$[-]$
1	2.6436	10.1675	0.9895	1.4199	30.0093	0.9948
2	1.2792	8.9620	0.9808	1.1807	18.9492	0.9953
3	1.3746	51.0054	0.9957	1.3380	45.0169	0.9728
4	1.8399	4.1488	0.9672	1.2149	15.9998	0.9144
5	5.5322	1.5748	0.9393	0.3875	51.3098	0.9390

TABLE 4. Fitting results of experimental data to model (1).

Location	t = 13 year			t = 20 year		
	D	J	r	D	J	r
	$[10^{-12}m^2/s]$	$[mg/(cm^2year)]$	$[-]$	$[10^{-12}m^2/s]$	$[mg/(cm^2year)]$	$[-]$
1	3.4547	3.1254	0.9892	1.7594	5.6885	0.9950
2	1.6311	1.9510	0.9813	1.4886	3.2192	0.9958
3	1.7736	11.3321	0.9956	1.9262	7.5512	0.9764
4	2.4768	1.0530	0.9680	1.5455	2.7413	0.9143
5	8.0252	0.6798	0.9483	0.4654	5.2835	0.9368

TABLE 5. Fitting results of experimental data to model (7).

Location	I_0	$\alpha\,(\%)$	
	$[kg/m^2]$	**Model (1)**	**Model (7)**
1	0.1520	28.6	23.5
2	0.1193	48.2	35.4
3	0.6483	18.3	32.0
4	0.1006	58.6	49.3
5	0.0645	33.9	26.8

TABLE 6. Parameter α values calculated for both models. See text for details.

Function	Laplace transform
$f(t)$	$F(s) = \mathcal{L}\left\{f(t)\right\}$
$af(t) + bg(t)$	$aF(s) + bG(s)$
a	a/s
t^n	$n!/n^{s+1}$
$\dfrac{d^n f(t)}{dt^n}$	$s^n F(s) - \sum\limits_{k=1}^{n}\left\{\left.\dfrac{d^{(k-1)}f(t)}{dt^{(k-1)}}\right|_{t=0} s^{n-k}\right\}$
$2\sqrt{\dfrac{t}{\pi}}\exp\left(-\dfrac{a^2}{4t}\right) - a\,\mathrm{erfc}\left(\dfrac{a}{2\sqrt{t}}\right)$	$s^{-3/2}e^{-a\sqrt{s}}$

TABLE 7. Laplace transforms used.

29

List of Figures

FIG. 1. Profiles calculated with (A) equation (1) and (B) equation (7).
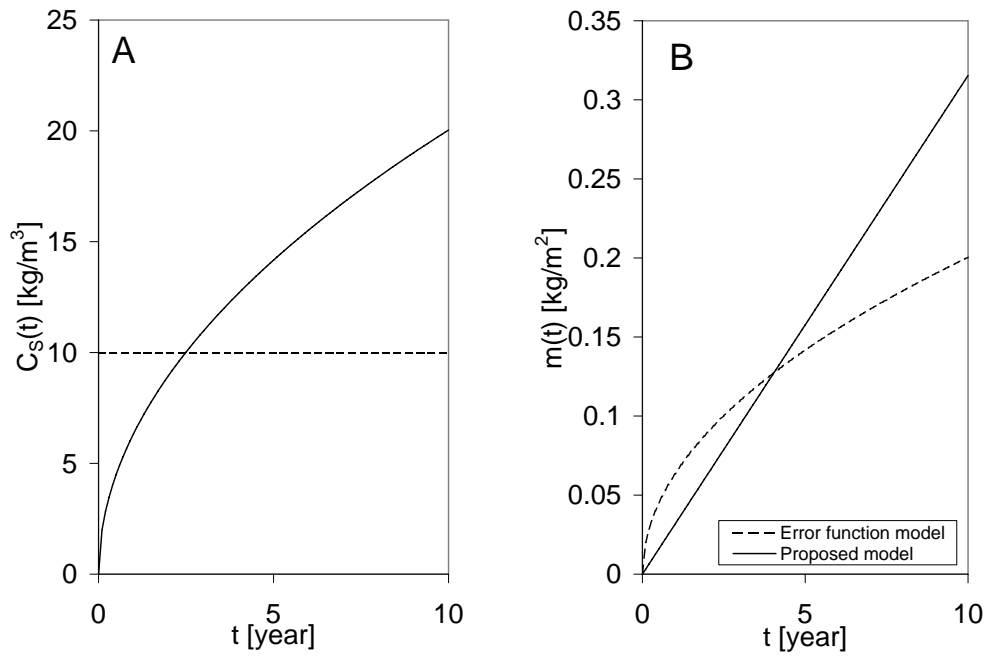
FIG. 2. (A) Surface concentration C_S, and **(B)** absorbed amount of chlorides m for the classical error function model (dotted line) and the proposed model (solid line).
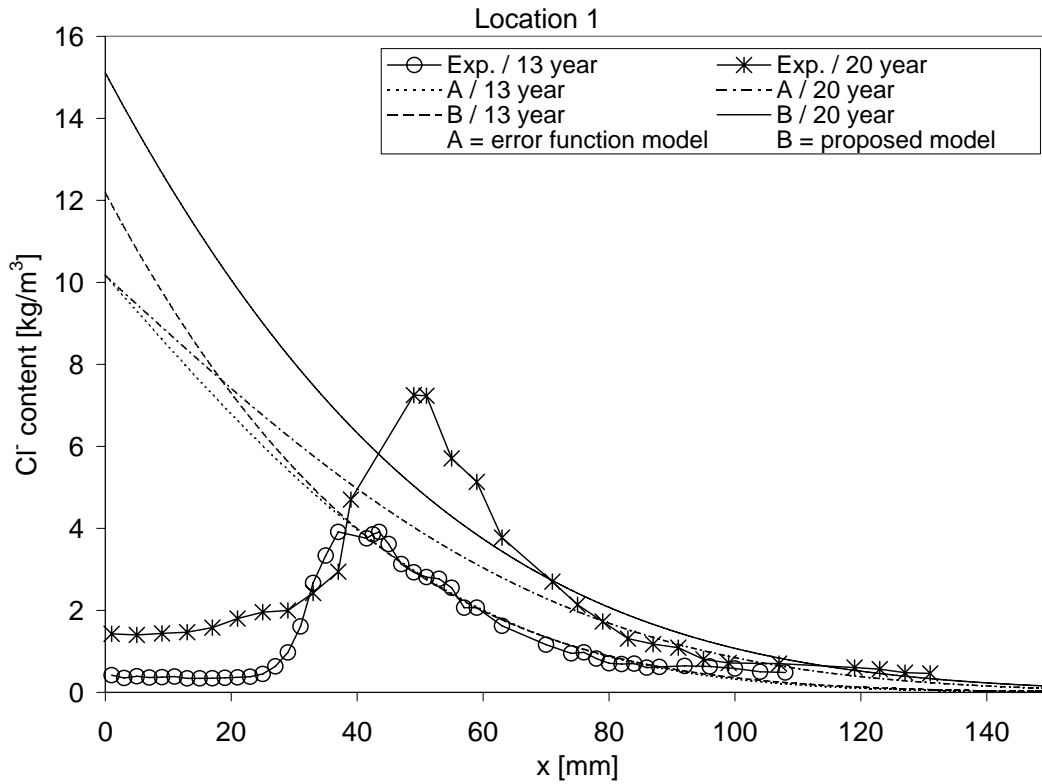
FIG. 3. Experimental and calculated chloride profiles for location number 1. A/20 year and B/20 year calculated with parameters fitted at 13 year. See text for details.
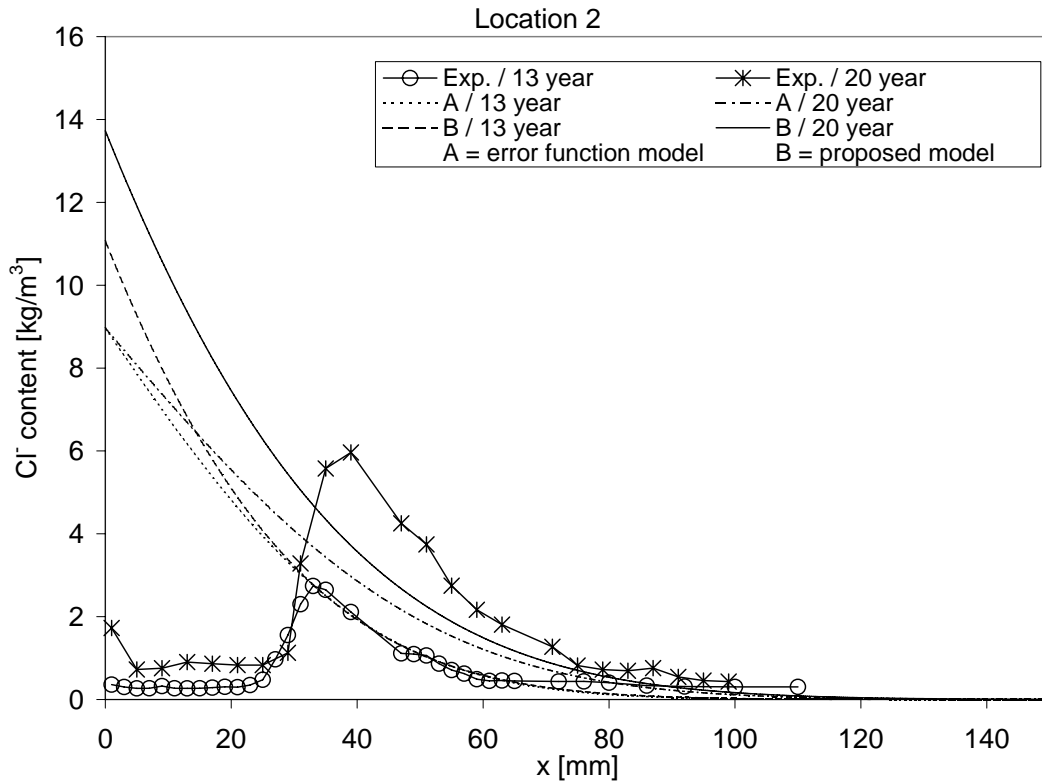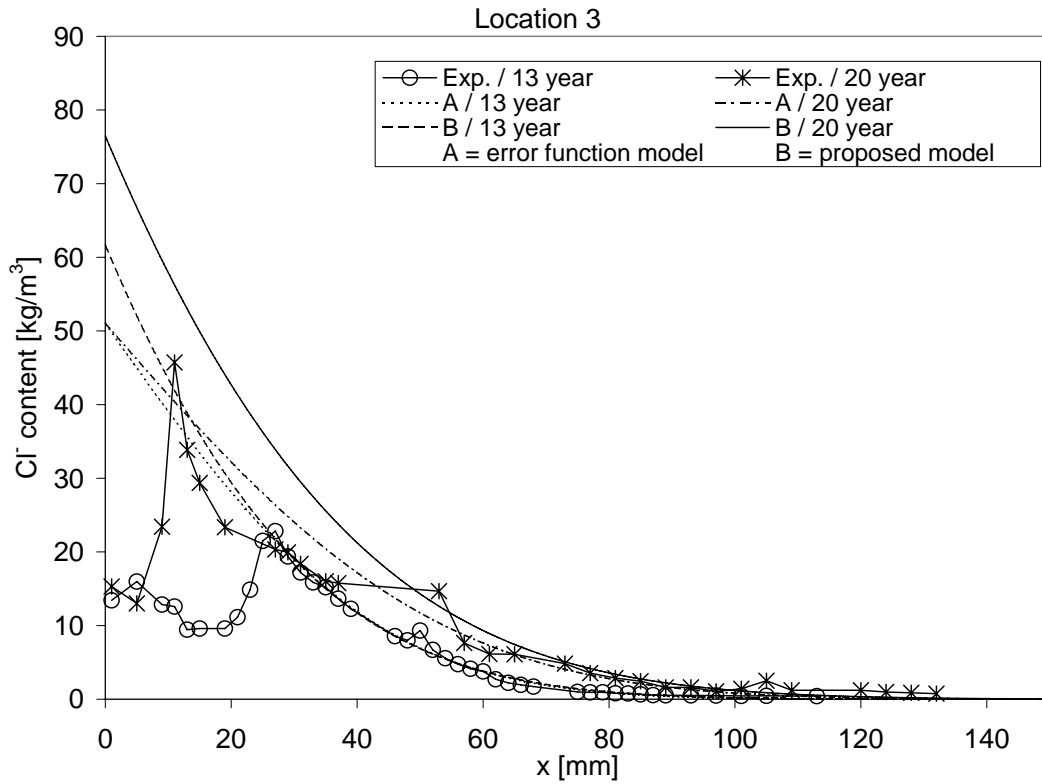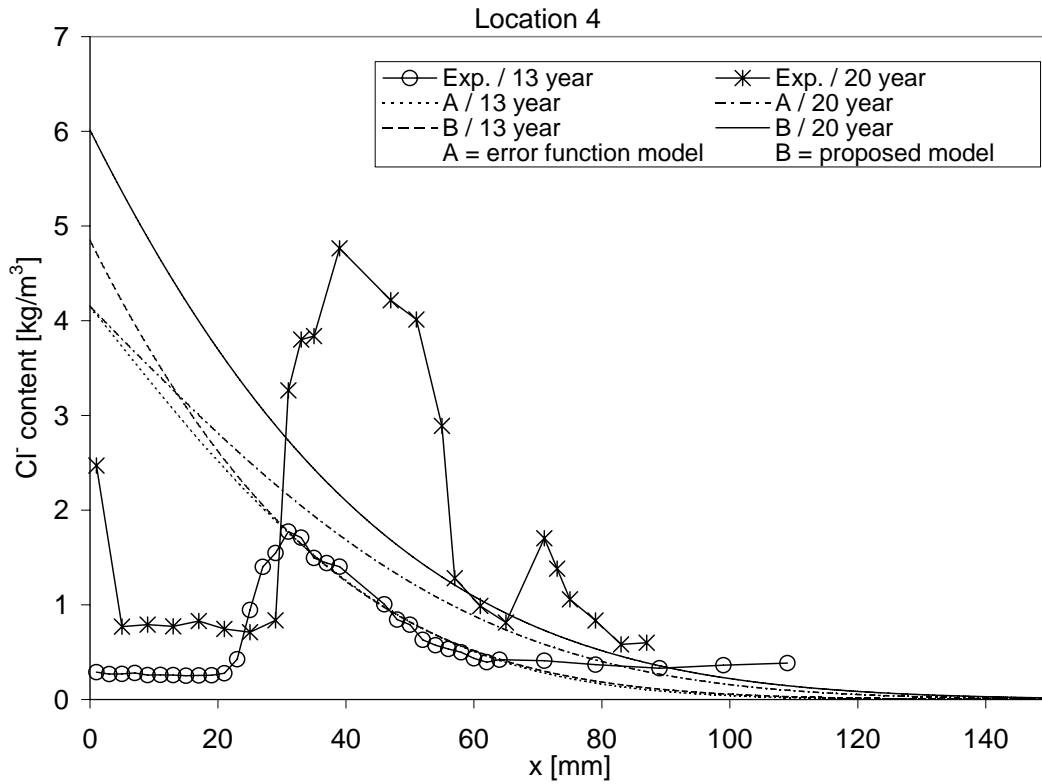
FIG. 4. Experimental and calculated chloride profiles for location number 2. A/20 year and B/20 year calculated with parameters fitted at 13 year. See text for details.
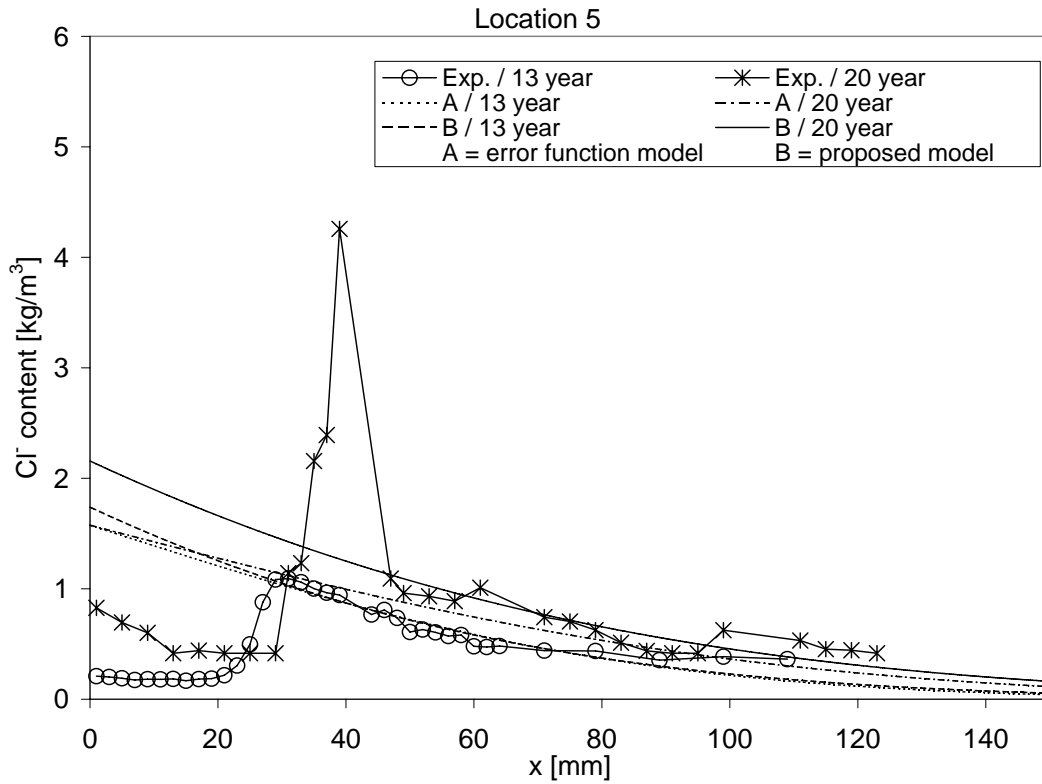
FIG. 5. Experimental and calculated chloride profiles for location number 3. A/20 year and B/20 year calculated with parameters fitted at 13 year. See text for details.

FIG. 6. Experimental and calculated chloride profiles for location number 4. A/20 year and B/20 year calculated with parameters fitted at 13 year. See text for details.

FIG. 7. Experimental and calculated chloride profiles for location number 5. A/20 year and B/20 year calculated with parameters fitted at 13 year. See text for details.
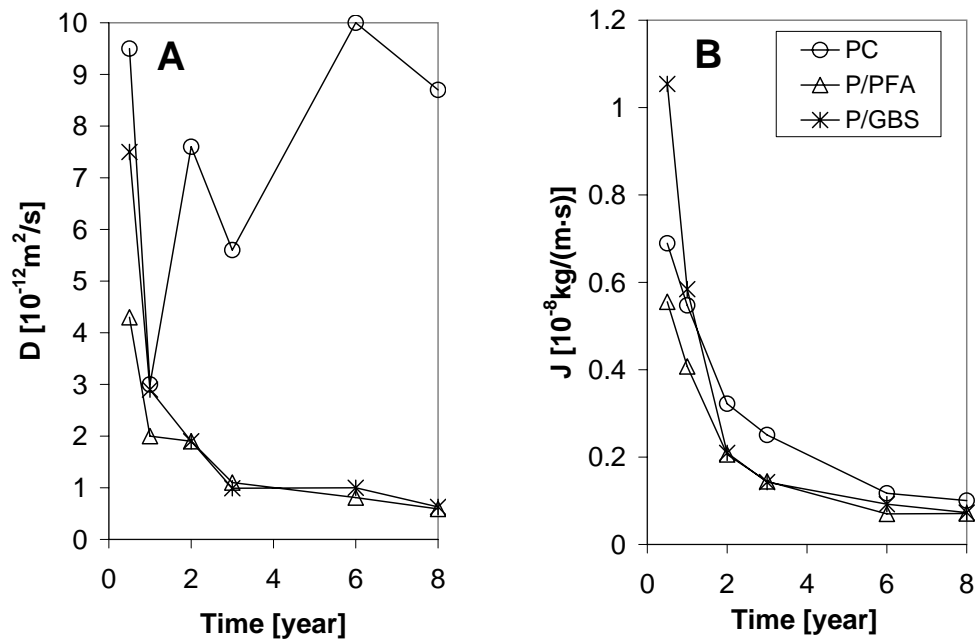
FIG. 8. (A) Diffusion coefficient against time, and (B) mean flux against time calculated from profiles. (Data from Thomas and Bamforth 1999)
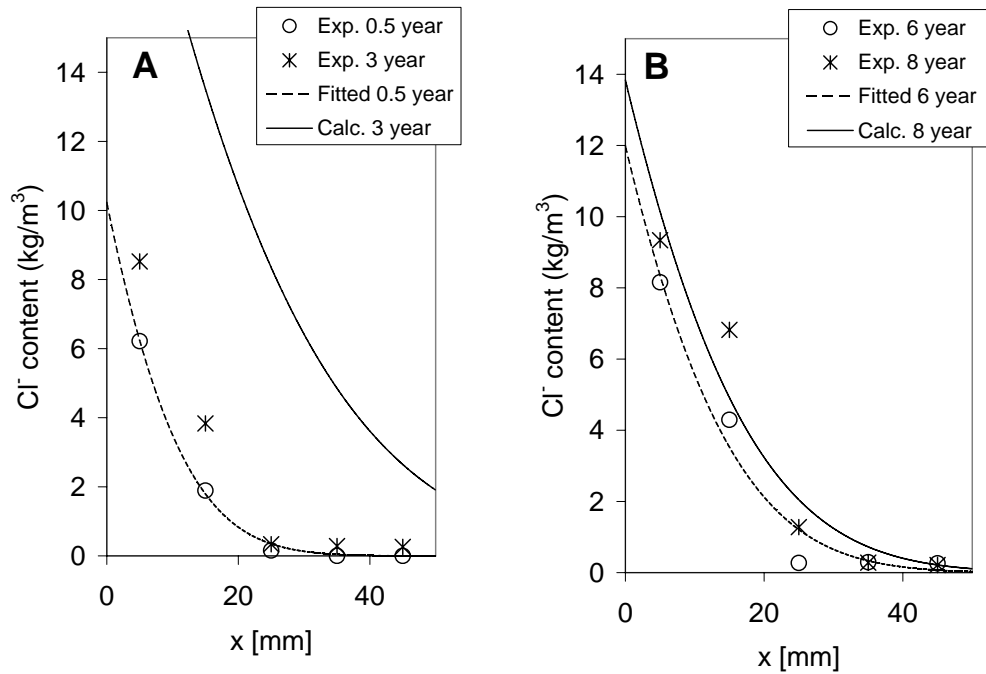
FIG. 9. Predicted profiles from a fitting compared with experimental profiles. (A) Fitted profile at 0.5 year and predicted profile at 3 year, and (B) fitted profile at 6 year and predicted profile at 8 year. (Data from Thomas and Bamforth 1999).